International Journal of Civil Engineering and Technology (IJCIET)
Volume 9, Issue 9, September 2018, pp. 1593–1610, Article ID: IJCIET_09_09_154
Available online at http://www.iaeme.com/ijciet/issues.asp?JType=IJCIET&VType=9&IType=9
ISSN Print: 0976-6308 and ISSN Online: 0976-6316

©IAEME Publication **Scopus** Indexed

COMPARISON OF 10 % AND 2/3 OF 2 % PE FOR 50 YEARS SEISMIC HAZARD AT YOGYAKARTA SPECIAL PROVINCE (YSP), INDONESIA CONSTRUCTED FROM THE PROBABILISTIC SEISMIC HAZARD ANALYSIS

Widodo Pawirodikromo*, Lalu Makrup, Mochammad Teguh, Bambang Suryo
Islamic University of Indonesia Yogyakarta, Indonesia

Eddy Hartantyo
Universitas Gadjah Mada, Indonesia
*Corresponding Author: widodo355@gmail.com

ANSTRACT

Indonesia is an area that is very vulnerable to the impacts of earthquake hazards, including in the Yogyakarta Special Province (YSP). According to [1] the earthquake hazards in particular area as well as the development of the Building Codes can be developed by carrying out the Probabilistic Seismic Hazard Analysis (PSHA) even though verifying the results as compare to the actual earthquake occurrence still need to be investigated. The seismic hazard map of the superseded Indonesian Seismic Codes was developed by applying 10 % Probability of Exceedance (PE) during 50 years, however, the current Codes was based on 2 % PE during 50 years. It is necessary to compare the PSA between two Codes. The probabilistic seismic hazard analysis (PSHA) at YSP with 10% and 2/3 of 2% PE for 50 years has been conducted. The PGA at the ground surface is done based on V_{S30} *published by USGS. The results of the analysis showed that by using more complete earthquake data, all PSA values obtained were slightly higher than the results as presented by [2] and PSA values of 2/3 of 2% PE are significantly greater than PSA based on 10% PE during 50 years.*

Key words: shallow crustal earthquake, megathrust, ground prediction equations, logic tree, probability of exceedance, probability seismic hazard analysis, peak ground acceleration maps, peak spectral acceleration maps.

Cite this Article: Widodo Pawirodikromo, Lalu Makrup, Mochammad Teguh, Bambang Suryo and Eddy Hartantyo, Comparison of 10 % and 2/3 of 2 % PE for 50 Years Seismic Hazard at Yogyakarta Special Province (YSP), Indonesia Constructed from the Probabilistic Seismic Hazard Analysis. *International Journal of Civil Engineering and Technology*, 9(9), 2018, pp. 1593-1610.
http://www.iaeme.com/IJCIET/issues.asp?JType=IJCIET&VType=9&IType=9

1. INTRODUCTION

Indonesia is a country that is prone to earthquake hazards. This was indicated by the occurrence of major earthquakes in the first decade of the 21st century starting from the M9.2 2004 Aceh earthquake, the M8.5 2005 Nias earthquake to the M6.3 2006 Yogyakarta earthquake and the M7.5, 2009 Padang earthquake. The most recent earthquakes that have occurred in Indonesia are the M6.4 July 29, 2018, Lombok earthquake and the M7.0 August 5, 2018, Lombok earthquake as well. These earthquakes are a result of Flores back-arc thurst activity that stretches from north of Flores island to the west until in the north of the Bali island as shown in Fig.1) [3,4].

The Yogyakarta Special Province (YSP) is one of 34 provinces in Indonesia. Based on the 2016 statistical data indicated that, the population of the YSP is 3720212 people living in the area of 6350.62 km2. Thus the population density at YSP is 585.8 people / km2. Based on Law No.56 / PRP / 1960, the population density in YSP which is more than 400 people/km2 falls in the "very dense" category of population density. Therefore, during the M6.3, 2006 Yogyakarta earthquake, the fatalities were very large/high, reaching more than 5500 people. By remembering such disasters, the earthquake disaster mitigation program is needed so that human fatalities in the future can be minimized.

There have been many earthquake disaster mitigation programs in YSP that have been planned and implemented. The seismic mitigation programs, in general, can be classified into 2-major activities i.e. physical and non- physical mitigation program. One of the non-physical mitigation programs is the availability of seismic hazard maps. In the superseded Indonesian Seismic Code, the spectral acceleration design in the seismic hazard map was based on 10% PE in 50 years or the building performance is targeted to perform up to Life Safety level [5]. However, in recent seismic Code, the spectral acceleration design is based on the seismic hazard of 2 % PE for 50 years multiplied by a factor of 2/3 in which the structure is targeted at least to reach the Life Safety performance. It is essential to evaluate these two approaches to ensure that the seismic load design will lead to structures that behave not only Life Safety but also reduce property losses [5].

Efforts to develop a map of seismic hazard in YSP have been carried out by [6]. Eighteen normal faults and six strike-slip faults were taken into account in the hazard analysis. The type and number of faults considered are very different from the type and number of faults used by [7]. The probabilistic seismic hazard package program EQRISK was used, and the annual rate of exceedance was represented by the earthquake return period. The earthquake return periods Tr = 10, 50, 100, 200, and 500 years were considered during the analysis. The maximum ground acceleration for the 200-year return period may reach 0.61-0.71g. However, the analysis was only based on 2-D seismic sources, only emphasized at Bantul district and the researchers themselves stated that the PGAs obtained were overestimated since the required sufficient data were not available.

Synthetic ground acceleration in Yogyakarta City based on the deagregation seismic hazards has been proposed by [8]. The probabilistic seismic hazard analysis (PSHA) approach was used by considering shallow crustal faults and subduction seismic sources. Because only 1-point is considered, the effect of shallow crustal and subduction earthquake remains separated / not combined until the matching acceleration time history in bed respectively for T = 0.2s and T = 1.0s. Ground surface time history is also obtained only 1-point which is calculated by vertically propagating shear waves from bedrock to the surface. The PSHA was carried out by considering 2 % probability during 50 years.

The peak ground acceleration (PGA) map of Yogyakarta city was presented by [9]. The PGA map was developed based on calculated PGA by applying 2-approaches: 1) the PGA is determined by using Kanai attenuation and 2) the PGA is calculated by conducting the vertical propagation of shear wave using NERA software in which 4-base rock time history with a particular value of PGA was used. Both of 2-approached was used in calculating PGA at 87 points comprising of 13-core drilling and 74 microtremor measurements. In addition, the maximum considered earthquake determined by the product between PGA taken from [10] and the site coefficient and the PGA calculated by using Boore et.al (1997) and Bozorgnia et.al.(2000) GMPE's were also presented. This study only limited for PGA map of the Yogyakarta city and determined by the deterministic method.

A comparison of 2-ground surface seismic hazards maps of the YSP has also been presented by [2]. The seismic hazard map was developed by using the 3-D Total Probability Seismic Hazard Analysis (PSHA). The shallow crustal and the subduction seismic sources were used. The bedrock seismic hazard maps were presented based on 10 % probability of exceedance during 50 years at fundamental period T = 0.2s and T = 1.0s. The first result is the surface seismic hazard map developed by the product between based rock seismic hazard map and the site coefficients at short period F_a and long period F_v published by UBC 1997. The second result is the surface seismic hazard map developed directly by using surface ground motion prediction equation (GMPE). The study was conducted based on the earthquake data up to 2013 and the 2007's family of Next Generation Attenuation (NGA).

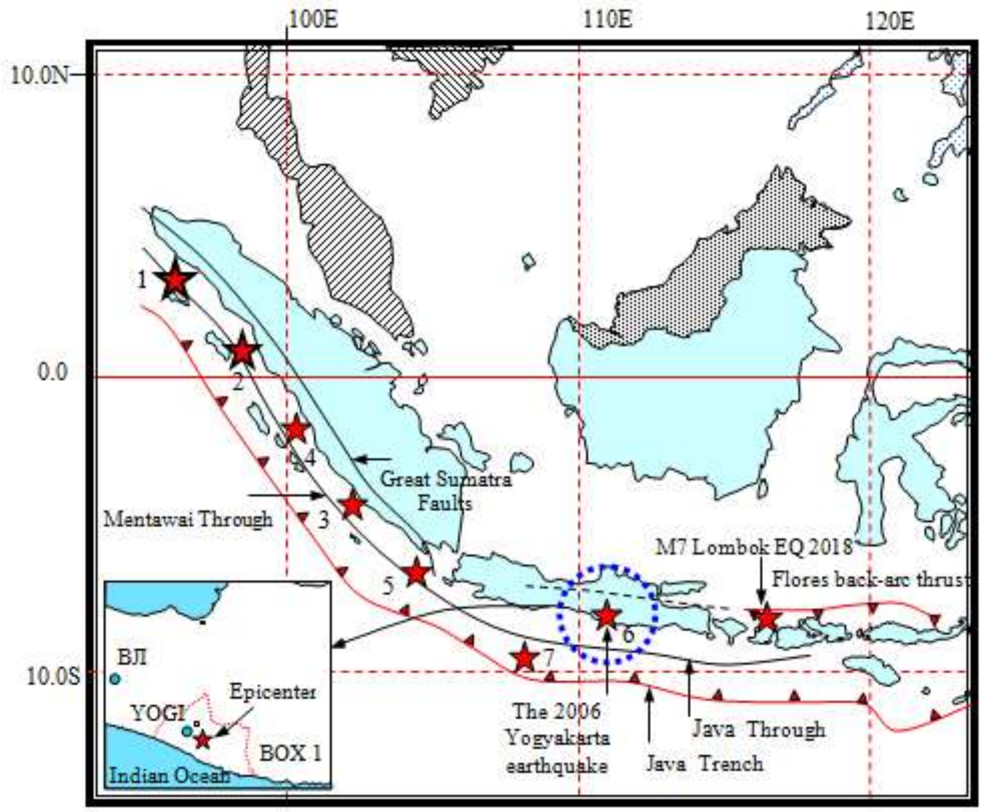

Figure 1 The 2006 Yogyakarta and the 2018 Lmbok earthquake

Several earthquakes with moderate magnitude have occurred around the Java island during the period of 2014 to 2017. On January 25, 2014, there was an earthquake with a magnitude of M6.5 in Kebumen. The coordinates of epicenter are 8.48S, 109.22E or 104 km south-west of Kebumen with a depth of 48 km. The earthquake has caused damage to buildings, particularly in Cilacap and Kebumen districts. On November 16, 2016, there was also occur an earthquake in Malang with a magnitude of M6.2 at a depth of 68 km. The coordinate of the epicenter is 9.32S, 113.12E or about 127 km south-east Malang city. On

December 15, 2017, an earthquake in Tasikmalaya with epicenter coordinates was 7.75S, 108.11E. The depth of the earthquake was 107 km and resulted in 4 fatalities.

All data on the above earthquakes have not been taken into account by [2]. Therefore, the aim of this study is to refine previous studies that have been carried out by [2,6,8,9] and to find out the difference of the hazard level for seismic design based on 10% and 2/3 of 2% PE for 50 years.

2. LOCAL GEOLOGY OF THE YOGYAKARTA SPECIAL PROVINCE (YSP)

As shown in Fig.2), the Yogyakarta Special Province (YSP) is located on the south coast of Java. Relative to the down-going Australian plate which moves northward, YSP is located in an overriding plate position. As a result of the down-going Australian plate movement that has lasted millions of years, land elevation has occurred in large parts along the southern coast of YSP. As a consequence of the location close to the Australian plate boundary, there is a series of volcanoes along the island of Java including Mount Merapi. Thus, YSP became an area which is stressed by the Australian plate down-going movement to the north and detained in the north by the Merapi volcano. Eventually, YSP became a depression area that would affect the tectonic activity in the region.

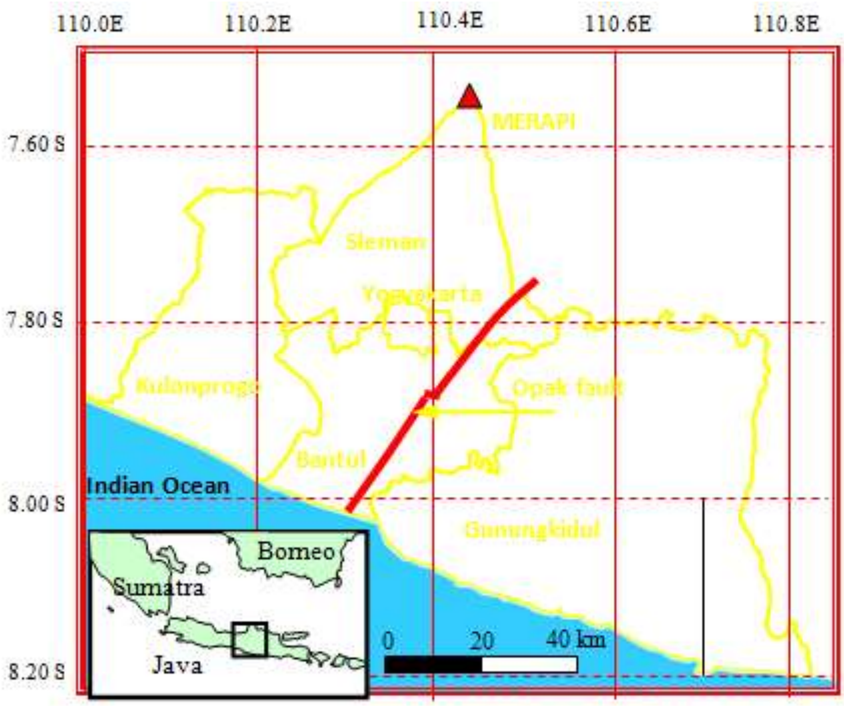

Figure 2 The local geology of Yogyakarta Special Province (YSP)

The formation of the rocks and soils in YSP were initiated during the Tertiary and Quarternary periods [11]. As clearly shown in the Fig.2) the western part of Kulonprogo and Gunungkidul districts are mountain ranges where the rocks were formed during the Tertiary period. In the northern part, i.e the Sleman regency (the closest to the slopes of the active volcano Mount Merapi), the soil profile consists mainly of coarse sand and gravel, formed by successive sedimentation from Mt. Merapi eruptions. Meanwhile, the southeastern parts, Kulonprogo and most of the Bantul district, are the valley areas where soils were formed during the Quarternary period. Their soil deposits are made up of fine sand, clay, and silt as a result of Tertiary sedimentary rock weathering [12]. It is clear in Fig. 2) that the existence of

Opak fault that triggered the Yogyakarta earthquake on May 27, 2006. The soil in these areas consists of relatively thick and young soil deposits, which have a high potential seismic vulnerability index [13].

3. EARTHQUAKE SOURCE MECHANISME

The YSP is located on Java island, Indonesia which is globally located on Eurasian Plate. Australian plate moves towards the north and subductions occur along the west of the island of Sumatra, south of Java and Nusatenggara and continue to turn in the Maluku islands. According to [14] the Australian plate moves collides and forms subduction of the Eurasian plate with a movement rate of approximately 5.4 mm / year. As a result, throughout the subduction zone there have been shallow earthquakes in the megathrust zone, and medium and deep earthquakes in the Benioff zone. These earthquakes become the past seismic data, while subduction activity has a potential to cause earthquakes in the future including in the YSP. Thus, seismic data in the subduction area must be used as a source and modeled for probabilistic seismic hazard calculations at YSP.

The direction of the movement of Australian plate with respect to Java island is almost perpendicular. As a result, buckling plates have occurred and resulted in active faults in particular places in Java including in the YSP. However, faults active in Java island did not occur massively as the Great Sumatra faults on the island of Sumatra. The active faults are the Cimandiri fault, Baribis fault and Lembang fault in West Java, Opak fault, Lasem fault and Pati Fault in Central Java and Kendeng fault mainly at east Java and partly at Central Java. There have been moderate and shallow earthquakes in the faults so that the seismic activity must be calculated and modeled as the shallow crustal earthquake in Probabilistic Seismic Hazard Analysis at the YSP.

4. PROBABILISTIC SEISMIC HAZARDS ANALYSIS

The probability of an earthquake occurring in the desired hazard parameters can generally be determined based on the principle of conditional probability. Based on this principle, the probability of an earthquake event with parameter X that exceeds an x value for an earthquake with magnitude m can be written to [15],

$$P(X > x) = P\left(X > x \middle| m\right) P_M(m) \tag{1}$$

Eq.1) basically is calculated based on an attenuation law. The probability of magnitude M parameters for certain values of P_M (m) will be related to the cumulative distribution function F_M (m). Meanwhile, according to [16] the relationship between probability density function f_M (m) with cumulative distribution function F_M (m) is,

$$f_M(m) = \frac{d}{dm} F_M(m) \tag{2}$$

Thus Eq.1) can be written to,

$$P_X(X > x) = \int_M P_X\left(X > x \middle| m\right) f_M(m)\ dm \tag{3}$$

Eq.3) is the probability of earthquake event based on particular attenuation and earthquake magnitude m. When the earthquake distance R is considered, then the probability of hazard parameter X exceeds an x value for a given magnitude M and distance R can be expressed in an integral form as,

$$P_X(X > x) = \int_M \int_R P(X > x | m, r)\ f_M\ f_R\ dr\ dm \tag{4}$$

M, m is erath quake magnitude, R,r is the earthquake distance, f_M and f_R respectively are the probability desity function of magnitude and distance.

Meanwhile the annual rate of exceedance for earthquake X parameters for a particular earthquake source can be determined through,

$$\lambda_X(x) = N.P_X(x) \tag{5}$$

Where N is the average number of earthquake events per year for earthquake magnitude ranging from m_o to m_{max} obtained from one of the earthquake source in the field.

For some potential earthquake sources that will affect seismic hazard at the site being reviewed, the annual rate of exceedance can be determined in the same way. If the number of potential earthquake sources is i = 1 ... n, then the total annual rate of exceedance $\lambda_X(x)$ is the contribution of all earthquake sources that can be written into,

$$\lambda_X(x) = \sum_{i=1}^{n} \lambda_{X,i}(x) = \sum_{i=1}^{n} N_i \int_M \int_R P_i\,(X > x \mid m, r)\; f_{M,i}\; f_{R,i}\; dr\, dm \tag{6}$$

For a 3-dimensional earthquake source, the probability of the occurrence of parameter X that exceeds the x value in Eq.1) must also take into account the influence of attenuation. Therefore, the effect of earthquake magnitude, distance and attenuation must be combined, so that Eq.6) becomes,

$$P_X(x) = \int_m f_M(m) \int_l f_{Lr}(l) \int_r P(X > x \mid m, r)\; f_{R|M,L_R,}(r, m, l)\; dr\, dl\, dm \tag{7}$$

In further, Eq.7) is used to modify the Eq.6) in terms of 3-D earthquake sources.

The annual rate of exceedance as presented in Eq.7) is calculated based on the pseudo-spectral acceleration (PSA) for a given T vibration period, so that a hazard curve can be made for each desired T period. Based on the hazard curve then uniform hazard spectrum can be made for each point under consideration. Thus bed-rock, short period and long period hazard map can be made.

5. METHOD OF INVESTIGATION

5.1. Earthquake Data

First of all is collecting earthquake source data with a radius of 500 km from the city of Yogyakarta based on the existing data base at USGS. The earthquake data collected is an earthquake that has a greater mo magnitude than M5 with a depth of less than 300 km. The earthquakes were then grouped into shallow crustal earthquakes, subduction earthquakes in megathrust zone and subduction earthquakes in the benioff zone.By using certain techniques in the statistics, the foreshock and aftershock earthquakes are separated by major earthquakes, so that the remaining earthquake is main-shock. The earthquake shock data was then transformed into an earthquake with the same magnitude, namely the moment magnitude Mw.

5.2. Earthquake Source Identification

It is necessary to identify all active faults at surrounding the YSP. The Cimandiri fault as presented in Fig.2) is a strike-slip fault [17] located at West Java along with the Cimandiri river. The Cimandiri fault with a strike of N70-80^o extends from the Gulf of Pelabuhan Ratu and passes through the Sukabumi, Cianjur and Bandung area. The Cimandiri fault is about 100 km length and undergoes slip-rate about 0.5-1.7 mm/year by [18], 4mm/year by [7], The Bumiayu fault located in the western part of Central Java is an extension of the Baribis fault located at the eastern end of West Java. Meanwhile, according to [19] the Bumiayu fault is reverse fault type. dip-slip 90^o and slip rate 2mm/year.

According to [20] the Lasem fault is an active fault starting from the eastern part of the city of Semarang towards the east through the northern mountains of Purwodadi and continues up to Lasem. Meanwhile, the Pati fault is a branch of the Lasem fault, continuing towards to the east at southern of Kudus and Pati town until near to Rembang. Data and parameter of Lasem and Pati faults are presented in Table 1.

Opak faults along the Opak river Yogyakarta were not well known before 2006. The Opak fault finally became the concern of the researchers after the May 27, 2006, Yogyakarta earthquake. According to [21] the 27th may 2006 Yogyakarta earthquake was caused by the activity of oblique Opak fault with strike-slip of 0.8m, dip-slip of –0.26m and strike N 48o to E. The slip-rate of Opak fault is about 2.4 mm/year with the maximum historical earthquake magnitude of Mw6.8 [7,22]. According to [23] the source mechanism of the 2006 Yogyakarta earthquake is the activity of the Opak fault with a dip angle of 87o; rake angle of 177^{o} (right lateral strike-slip) and the upper edge of the fault (Z_{TOR}) at 6 km. The Opak, Lasem, Pati, and Bumiayu faults are the active faults that are taken into account in this analysis.

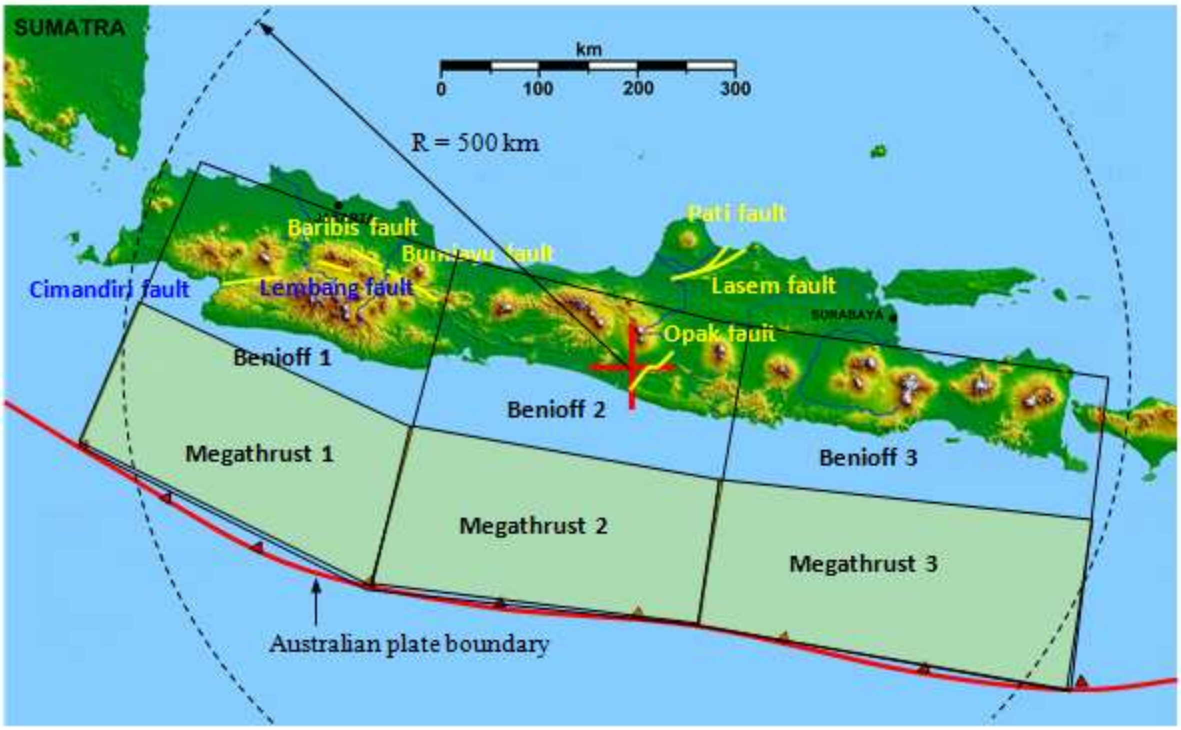

Figure 3 The earthquake source mechanism of the YSP.

Table 1 The data and parameter fault in Yogyakarta and Central Java [7,8]

No	Fault	Location	Slip-rate	Source mechanism	Fault length	M_{max}
1	Opak-Yogya	Yogyakarta	2.4 mm/year	right strike-slip	31.6 km	6.8
2	Lasem	Central Java	0.5 mm/year	Strike -slip	114.9 km	6.6
3	Pati	Central Java	0.5 mm/year	Strike slip	51.4 km	6.8
4	Bumiayu	Central Java	0.5 mm/year	right strike-slip	44 km	6.0
5	Cimandiri	West Java	2.0 mm/year	Strike-slip	98 km	7.2
6	Baribis	West java	0.2 mm/year	Strike-slip	64 km	6,8
7	Lembang	West Java	2.0 mm/year	Strike-slip	30 km	6.6

Meanwhile, the earthquake source mechanism caused by subduction activity of the Australian Plate is presented in Table 2. Within a radius of 500 km from the city of Yogyakarta, the subduction seismic source mechanism is divided into 3 zones consisting of

Megathrust and Benioff source models. According to [7, 24], subduction activity in the south of the island of Java has a potential to cause a maximum earthquake of Mw8.1.

Table 2 Source model of Subduction earthquake mechanism

No.	Source Model	Zone		
		Zone-1	Zone-2	Zone-3
1	Megathrust	Megathrust-1	Megathrust-2	Megathrust-3
2	Benioff	Benioff-1	Benioff-2	Benioff-3

5.3. The Ground Motion Prediction Equation (GMPE)

The ground motion prediction Equation (GMPE) is one of the important instruments used in PSHA. In general, GMPE an earthquake parameter is stated in an equation that contains 3 main components, namely the source, transmission path and site effects [25]. The GMPE is used to predict earthquake parameters such as acceleration, velocity, and displacement, or can be expressed in term of spectral displacement (SD), pseudo-spectral acceleration (PSA) or pseudo spectral velocity (PSV). Take care must be taken in selecting the GMPE, particularly to meet the required criteria. The general and detailed criteria for selecting and adjusting the GMPE models have been presented briefly by [26,27]. Among the general criteria is to consider global earthquake models and exclusion criteria. According to [26,28,29] the exclusion criteria in the selection of the GMPE it should be considered in the PSHA and the criteria have been summarized by [30].

Given the earthquake source mechanism as stated above is mainly shallow crustal and subduction earthquakes, then the GMPE used must also follow the types of its earthquake source mechanism. Considering that GMPE derived based on earthquake data in Indonesia is not available, then the GMPE from other countries is used that matches the earthquake source mechanism in YSP. The GPME used for modeling the parameter of shallow crustal earthquake in YSP are: a) Boore, Joyner and Fumal (1997); b) Sadigh et.al. (1997); c) the Atkinson and Boore (2006); d) Campbell and Bozorgnia (2006); e) Chiou and Young (2006); f) Boore and Atkinson (2007) and g) Abrahamson and Silva (2007).

5.4. Epistemic Uncertainty and Logic Tree

The ground motion prediction equation (GMPE) is commonly presented in terms of median spectral amplitudes including its intrinsic uncertainties. In general, there are 2 types of intrinsic uncertainties that have been agreed by researchers, namely epistemic and aleatory uncertainties [31-33]. The epistemic uncertainty can be caused by an incomplete knowledge which can consist of several things i.e. inexact model selection, error in statistics, error in measurements and errors in the database. In probabilistic seismic hazard analysis (PSHA) the presence of epistemic uncertainty can be treated by applying the logic tree model [34]. Meanwhile, aleatory uncertainty in another side may be caused by the natural variability of the soil site, the soil non-linearity or site amplification [32] usually consists of intra and inter-events [35] and presented by standard deviation or sigma [26].

According to [36], there are several important aspects that must be considered in preparing the logic tree, namely: 1) GMPE candidates must not be included in exclusion criteria; 2) GMPE candidates must be worldwide and in accordance with the type of tectonic regimes; 3) there is a match between the earthquake magnitude range that occurs in the site with the GMPE and 4) GMPE must be presented in a fairly long frequency range. Given that there are many uncertainties in predicting earthquake parameters, probabilistic seismic hazard analysis is generally used by many GMPE candidates who have been grouped according to the type of tectonic regimes. To increase objectivity and ranking, each GMPE candidate is assessed through expert judgment and tested through procedures such as presented by [37]. Finally, the weighting factor is given to GMPE candidates based on the result of ranking and expert judgment that has been decided. Based on all important aspects as stated above, the logic tree in probabilistic hazard analysis in the YSP is as presented in Figure 5.

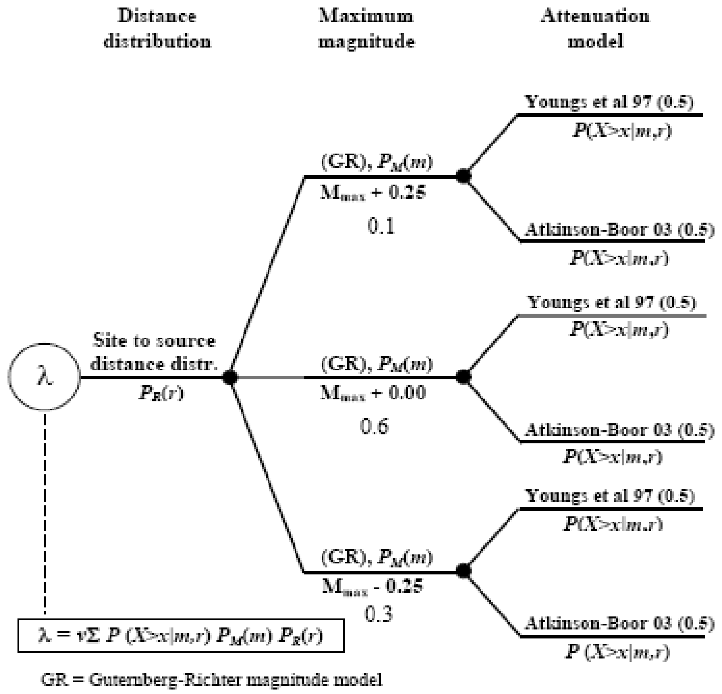

Figure 4 The Logic Tree for subduction earthquake source

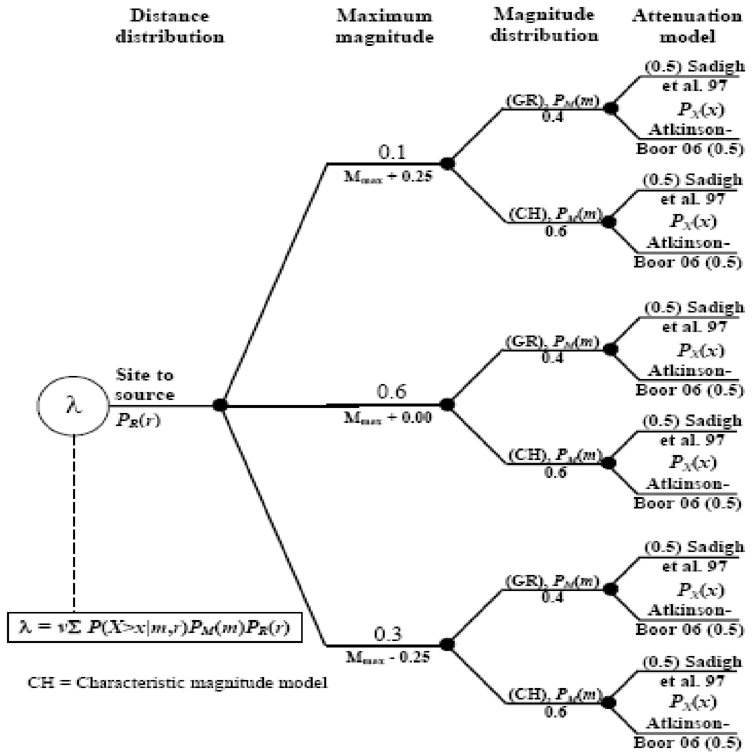

Figure 5 The Logic Tree for the shallow crustral earthquake source

6. RESULTS AND DISCUSSIONS

6.1. PGA at bed-rock and PGA at Ground Surface

The peak ground acceleration (PGA) map of the Yogyakarta Special Province (YSP) computed based on a 10 % probability of exceedance (PE) during 50 years lifetime is presented in Fig.6). This happens because according to [13] the maximum depth of soil deposits occurs in Opak river valley. It is clear in the figure that the maximum PGA is 0.5g which is located along the Opak fault trace or Opak river. In the figure, also shows that the maximum PGA orientation also follows the orientation of the Opak fault.

Meanwhile, the PGA map at ground surface computed from PHSA based on VS30 by USGS is presented in Fig.7). It is clearly depicted in the figure that the maximum surface PGA is 0.60g and also occurs along the Opak fault. Thus, as compared to the base-rock, hence, there was soil amplification as high as 1.20. In addition to occurring along the Opak river, the PGA amplification also extends particularly in the middle of Gunungkidul district. It can also be seen in Fig.6) and Fig.7) that the PGA distribution patterns at base-rock and ground surface are not exactly same. This condition will affect the distribution of site coefficient at T = 0 or F_{PGA}.

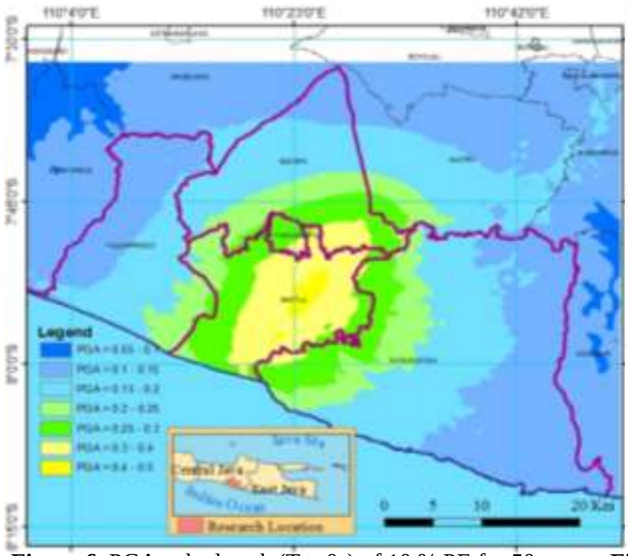

Figure 6. PGA at bed-rock (T = 0s) of 10 % PE for 50 years

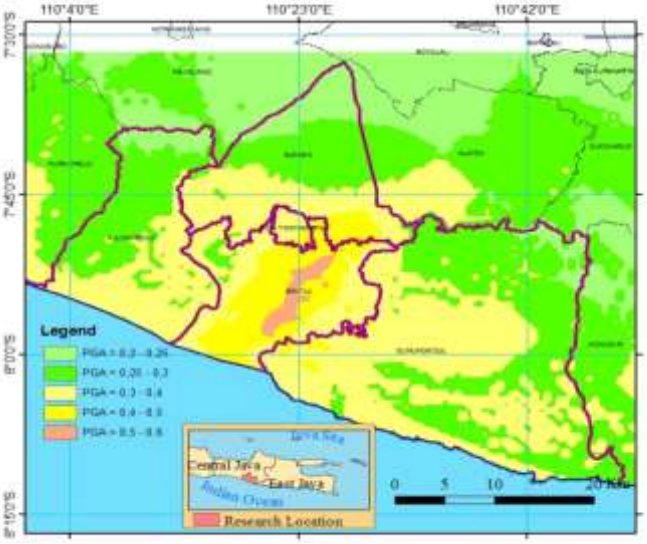

Figure 7, PGA at gr. surface (T = 0s) of 10 % PE for 50 years

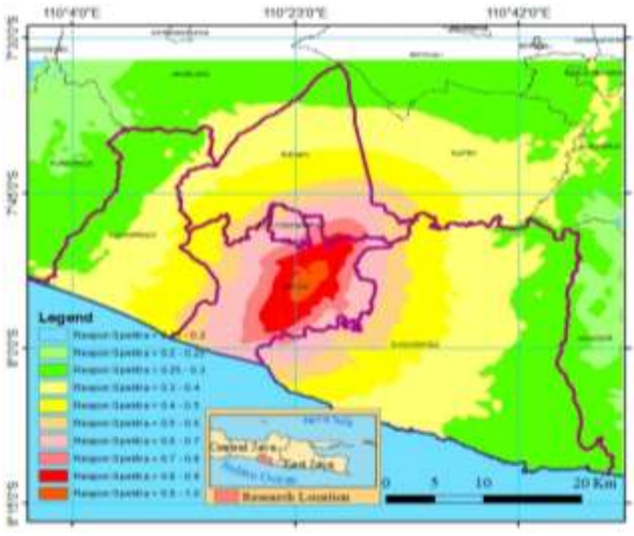

Figure 8. PSA at bed-rock (T = 0.2s) of 10 % PE for 50 years

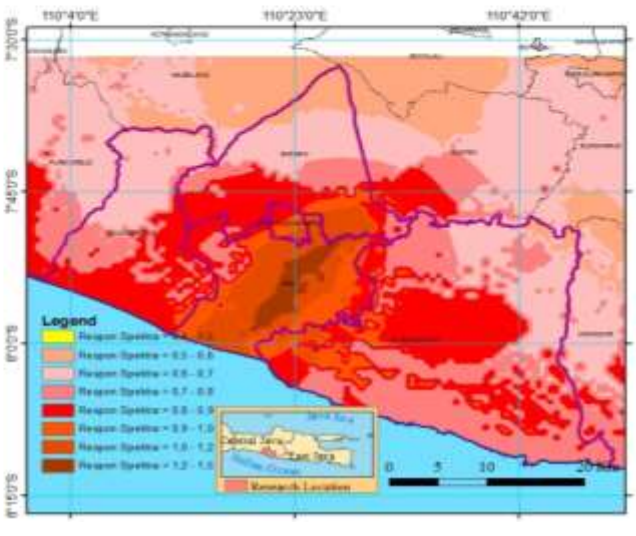

Figure 9 Surface PSA (T = 0.2s) of 10 % PE for 50 years

Meanwhile, the peak spectral acceleration (PSA) at base-rock at period T = 0.2s of the 10 % PE over the 50 years is presented in Fig.8). By comparing between Fig.6) and Fig.8), it is clear that the pattern of PGA at base-rock (T = 0.0s) is relatively similar to PSA distribution at base-rock in the period of T = 0.2s. The value of the maximum PSA is about 1.0g and still occurs along the Opak fault/river. Meanwhile, the PSA at ground surface for T= 0.2s is as shown in Fig.9) or with respect to base-rock has occurred soil amplification as high as 1.50.

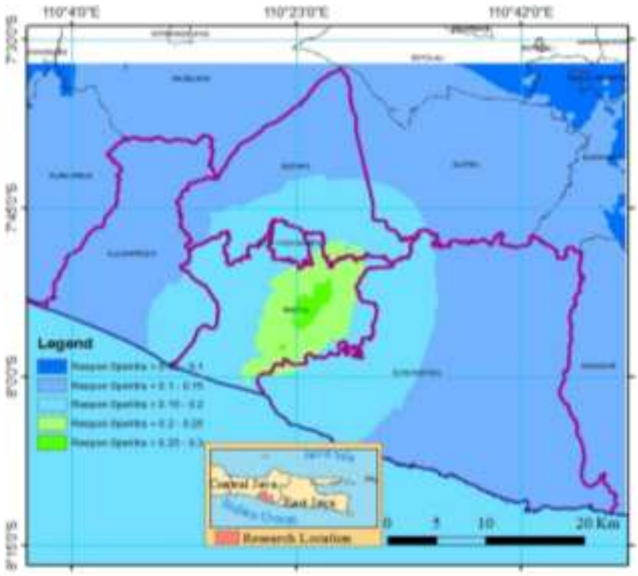

Figure 10. PSA, T = 1.0 dt, batuan dasar, 10 %, 50 th

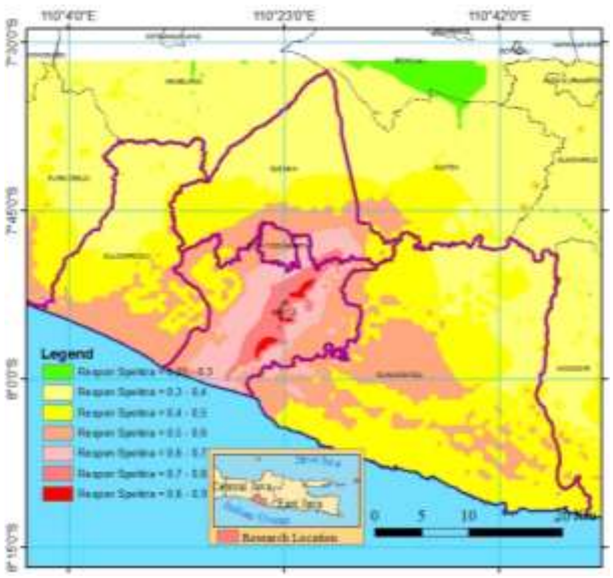

Figure 11. PSA, T = 1.0 dt, permukaan, 10 %, 50 th

At Fig.11 is presented the base-rock PSA for period T = 1.0s based on 10 % PE during 50 years, in which the maximum PSA is about 0.30g much less the PSA at T = 0.2s as high as 1.0g. In line with previous results, the PSA dan PGA distribution patterns in bed-rock and ground surface which has period T = 0.2s and T = 1.0s are almost the same. The maximum PSA for T = 1.0s is about 0.80-0.90g or has amplified about 2.67- 3.0 as compared to PSA at bed-rock.

6.2. Comparison between 10 % and 2/3 of 2 % PE during 50 years

Fig. 12 is actually the same as Fig.6 but is shown again to be compared with the 2/3 of 2% PE over 50 years as shown in Fig.13. The maximum PGA at bed-rock in Fig.12) is about 0.40 - 0.5g, meanwhile the maximum PGA at bed-rock in Fig.13) is about 0.50 - 0.60g. Thus, PGA ar 2/3 of 2% PE over the 50 years is about 20 - 25 % greater than PGA for 10% PE for 50 years. In addition to being bigger, the distribution of PGA for 2/3 of 2% PE for over 50 years is also wider, even though its pattern is still similar.

Meanwhile, Fig.14 is surface PGA map for 10% PE over 50 years and Fig.15 is the surface PGA map for 2/3 of 2% PE during 50 years. The maximum surface PGA at Fig.14) is about 0.5 - 0.60g, while the maximum surface PGA at Fig.15 is about 0.70 - 0.80g. Therefore, aside from wider distribution the maximum PGA of 2/3 of 2% PE during 50 years is also approximately 20 - 33 % greater than maximum PGA of 10 % PE for over 50 years. In line with previous results, the maximum PSA value occurs along the Opak fault as presented in Fig. 2).

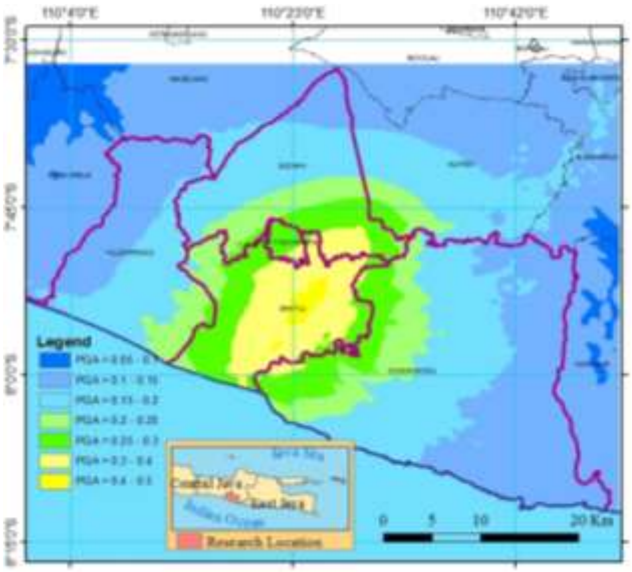

Figure 12. PGA at bed-rock (T = 0s) of 10 % PE for 50 years

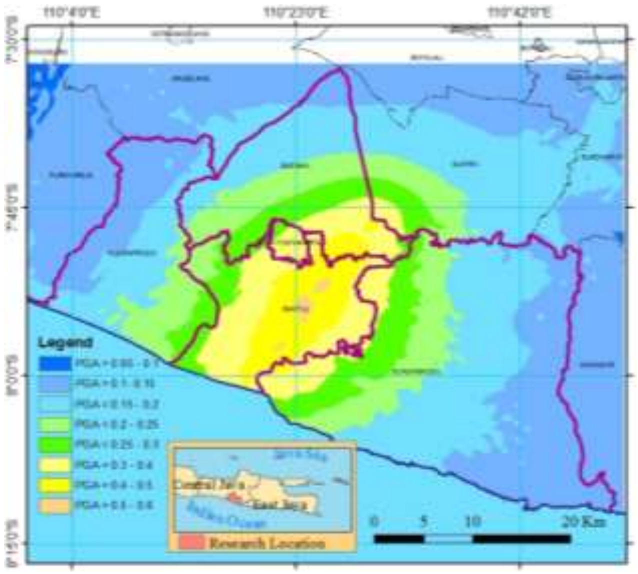

Figure 13 2/3 of bed-rock PGA at 2 % PE over 50 years

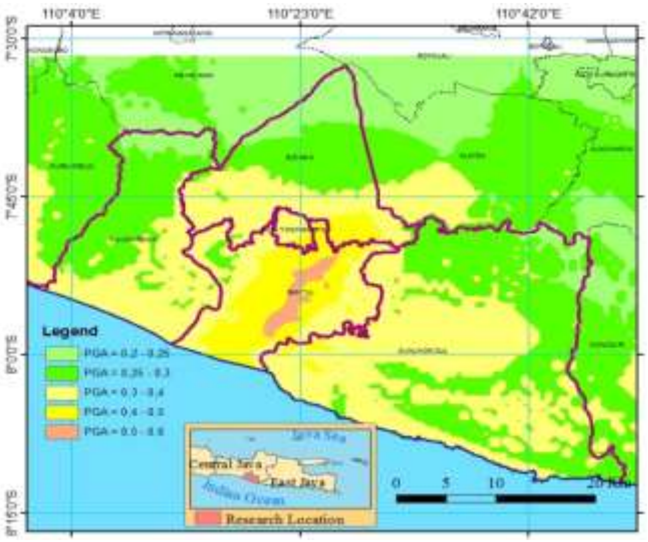

Figure 14 Surface PGA (T = 0s) of 10 % PE for 50 years

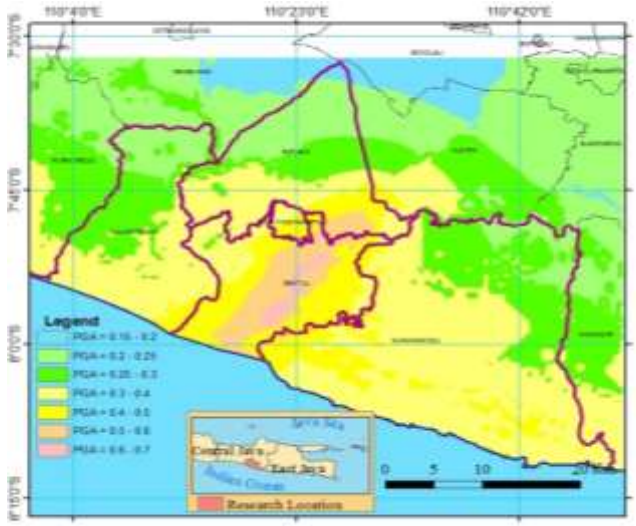

Figure 15 2/3 of surface PGA at 2 % PE over 50 years

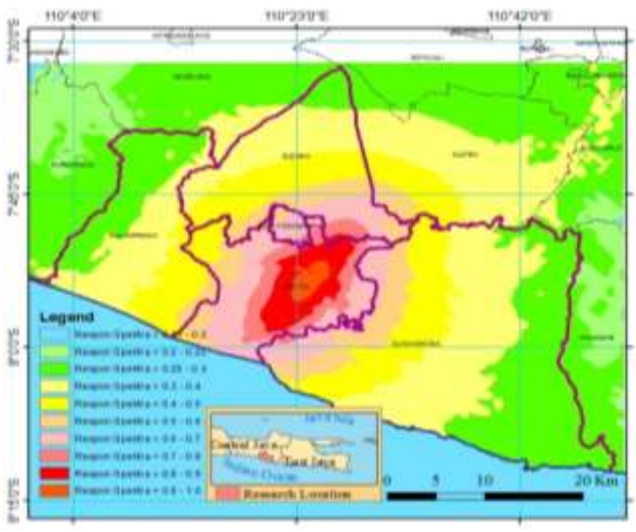

Figure 16. PSA at bed-rock (T = 0.2s) of 10 % PE for 50 years

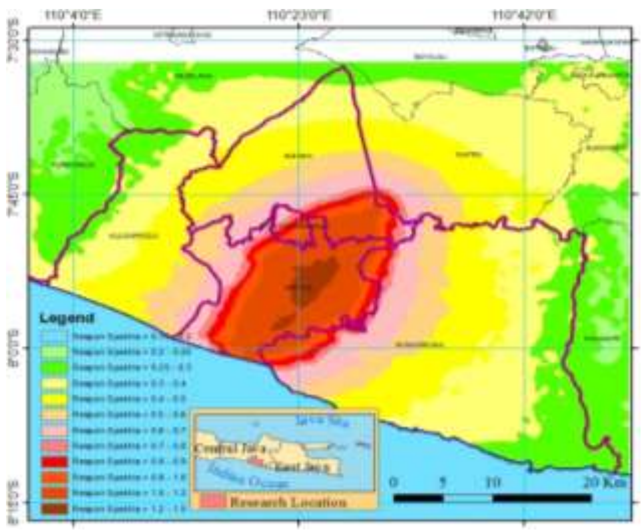

Figure 17. 2/3 bed-rock PSA (T= 0.2s) of 2 % PE for 50yrs

Fig. 16) is the same as Fig.8 which is shown again, namely PSA in bed-rock at T = 0.2s for 10% PE for 50 years. Fig. 16) is compared with 2/3 PSA in bed-rock for 2% PE for 50 years in the same period that is T = 0.2s as presented in Fig.17). In Fig. 17) it appears that in general the distribution of PSA is similar to that of FIg.16 and it only spreads to a wider area. It appears in Fig. 17) that the maximum PSA reaches a value of 1.2 - 1.5, while in Fig.16 it only reaches 0.9 - 1. Thus the value of 2/3 PSA for 2% PE is 33 – 50 % greater than PSA for 10% PE for 50 years. Since the maximum PSA value always occurs along the Opak fault, it can be concluded that fault earthquake source or shallow crustal earthquake dominates the PGA or PSA values in YSP.

Fig. 18) is the surface PSA map for period T = 0.2s in 10% PE for 50 years and is actually the same as Fig. 9. Meanwhile Fig. 19 is a map of 2/3 of 2% PE over a period of 50 years. In line with previous results, the pattern of PSA distribution on the ground surface for 2/3 of 2% PE for 50 years in Fig. 19) is similar to the distribution of PSA on the surface for 10% of PE for 50 years as presented in Fig. 18) but with a wider area of PSA distribution. Thus PSA for 2/3 of 2% PE is 25-33% greater than the maximum PSA at 10% PE for 50 years.

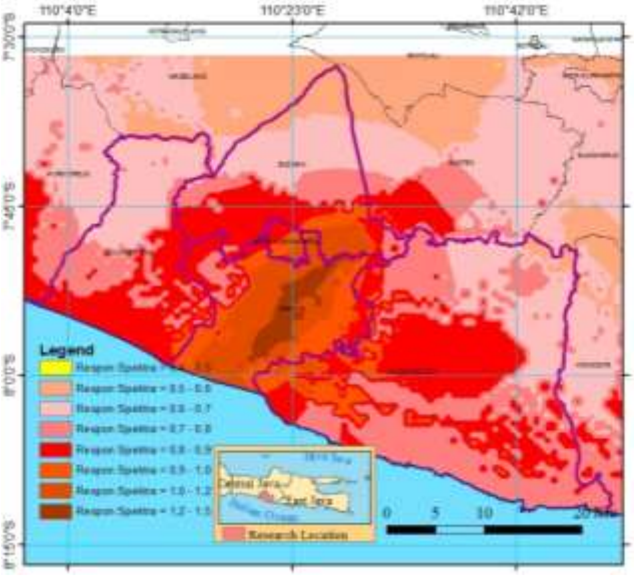

Figure 18. Surface PSA (T = 0.2s) of 10 % PE for 50 years

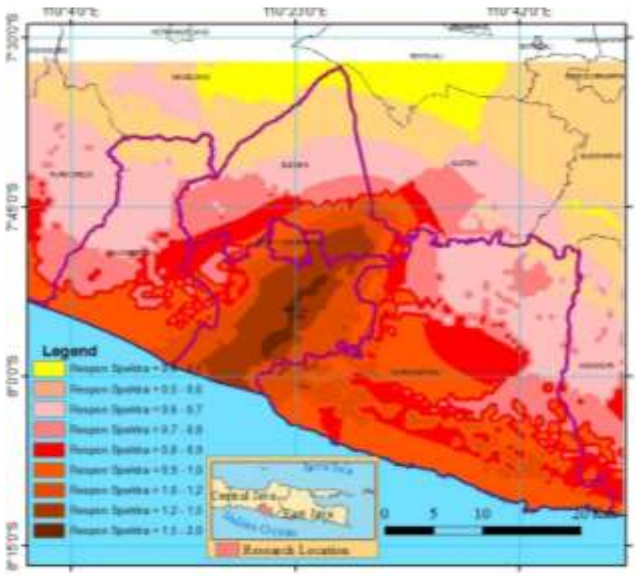

Figure 19 2/3 surface PSA (T= 0.2s) of 2 % PE for 50yrs

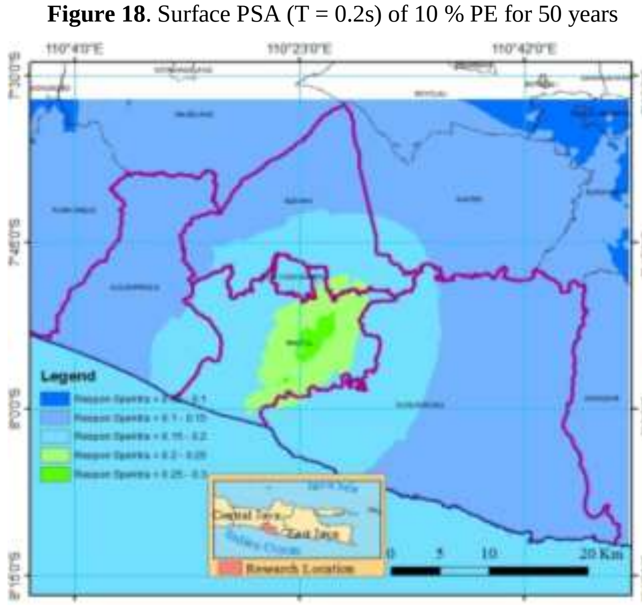

Figure 20. bed-rock PSA (T = 1.0s) of 10 % PE for 50 years

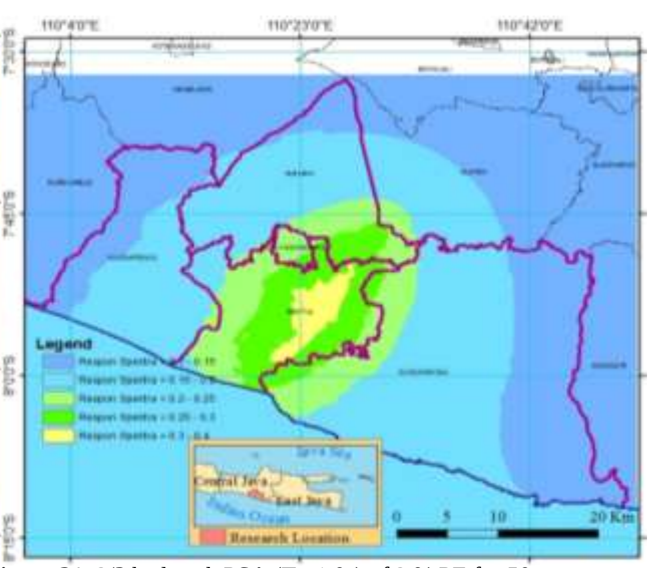

Figure 21. 2/3 bed-rock PSA (T= 1.0s) of 2 % PE for 50yrs

Fig.20) is the PSA map in bed-rock for the period T = 1.0s at 10% PE for 50 years, which is the same as Fig. 10). Meanwhile Fig.21) is a PSA map for 2/3 of 2% PE over the period of 50 years. Again, building PSA for 2/3 of 2% PE for 50 years is similar to the PSA distribution for 10% PE for 50 years, the only difference being that the PSA spreads over a wider area. If in Fig.20) the maximum PSA value ranges from 0.25-0.30, while the maximum PSA value in Fig. 21) ranges from 0.30m-0.40. This means that the maximum PSA value at 2/3 of 2% PE is 20-33% greater than the maximum PSA value for 10% PE ever 50 years.

Fig.22) is a PSA map on the surface at T = 1.0s from an analysis of 10% PE for 50 years which is actually the same as Fig. 11. Fig. 22) will be compared with the PSA map of 2/3 of 2% PE for 50 years as presented in Fig. 23). In both pictures, it appears that the maximum PSA orientation follows the direction of the Opak fault as presented in Fig. 2). Again these results indicate that the presence of Opak faults has a very strong influence on the PGA and PSA maps on YSP. The maximum PSA value in Fig. 22) is in the range of 0.80 - 0.90g, while the maximum PSA in Fig. 23) is in the range of 1.0 - 1.20g. Thus, 2/3 of PSA 2% PE for 50 years is 20-33% greater than PSA from 10% PE for 50 years.

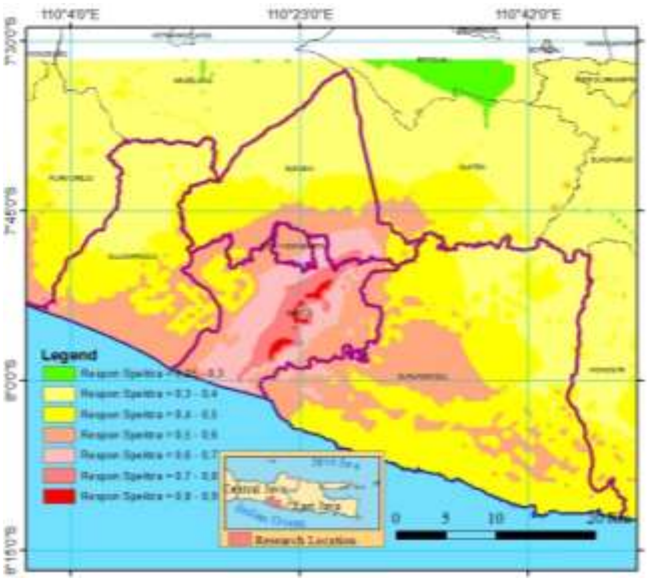

Figure 22. Surface PSA (T = 1.0s) of 10 % PE for 50 years

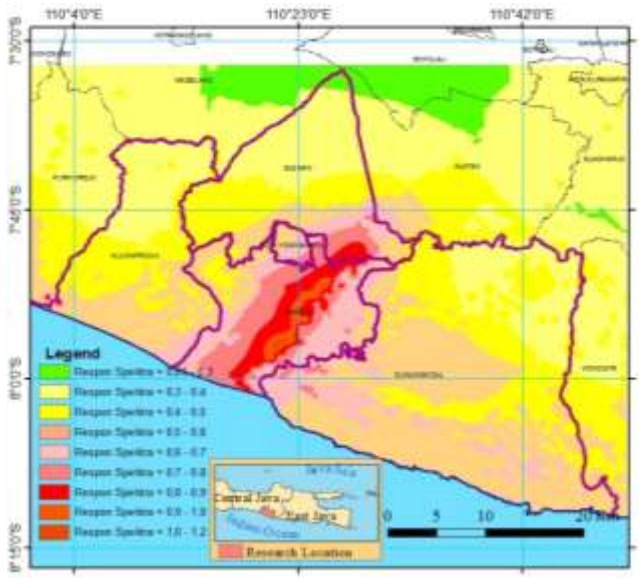

Figure 23. 2/3 surface PSA (T= 1.0s) of 2 % PE for 50yrs

The summary of PSHA analysis in bed-rock and on the surface of 10% PE for 50 years is presented in Table 3. It appears in the table that the PGA and PSA ratios between the surface against the bed-rock bed are close to the site coefficient values at T = 0 or F_{PGA}, in the short period or F_a and in the long period or F_v. The ratio between the two appears to be greater in the higher T period. This is similar to that stated by [37-38] that the soil amplification tends to be greater in the larger T period and the smaller bedrock acceleration. Between site coefficients F_a and F_v with soil-amplification is actually not the same, because GMPE used in the PSHA has not taken into account the depth of the soil deposits.

Table 3 PGA , PSA and its ratio for 10 % PE during 50 years

Level and Ratio	T = 0.0s	T = 0.20s	T = 1.0s
	PGA (g)	PSA (g)	PSA (g)
Surface (S)	0.50 – 0.60	1.20 – 1.50	0.80 – 0.90
Bed-rock (B)	0.40 – 0.50	0.90 – 1.0	0.25 – 0.30
Ratio S/B	1.20 – 1.25	1.33 – 1.50	3.0 – 3.20

Table 4 Comparison of maximum PGA and PSA computed from 10 % PE and 2/3 of 2% PE over 50 years

Level	Period T = 0.0 s		Period T = 0.20 s		Period T = 1.0 s	
	10 % PE	2/3 of 2 % PE	10 % PE	2/3 of 2 % PE	10 % PE	2/3 of 2 % PE
	PGA (g)	PGA (g)	PSA (g)	PSA (g)	PSA (g)	PSA (g)
Surface	0.50 - 0.60	0.70 - 0.80	1.20 - 1.50	1.50 - 2.0	0.80 - 0.90	1.0 – 1.20
	Difference : 20 – 33 %		Difference : 25 – 33 %		Difference : 25 – 33%	
Bed-rock	0.40 – 0.50	0.50 – 0.60	0.90 – 1.0	1.2 – 1.50	0.25 – 0.30	0.30 – 0.40
	Difference : 20 – 25 %		Difference : 30 – 50%		Difference : 20 – 33%	

Meanwhile, the comparison between PGA and PSA for both bed-rock and on the surface for 10% PE and 2/3 of 2% PE for 50 years is presented in Table 4. In Table 4 appears that PGA and PSA for 2/3 of 2% PE are all greater than PGA and PSA for 10% PE for 50 years. In general, the maximum values of 2/3 of 2% PE are around 20-33% greater than PGA and PSA from 10% PE for 50 years. Thus, the spectral acceleration used in determining strength demand at the Seismic Code based on 2/3 of 2% PE for 50 years is approximately 20-33% greater than the design strength of the superseded Code based on the target Life Safety performance from 10% PE for 50 years. However, these results still need to be investigated more broadly and deeply in the future.

7. CONCLUSIONS

Maps of peak ground acceleration (PGA) and peak spectral acceleration (PSA) in YSP with 2 different approaches have been made through the Probabilistic seismic hazard analysis. The results of the analysis of the two approaches have been placed side by side and then to be compared. In connection with these results above, it can be concluded as follows.

- Although the earthquake source mechanisms used in this study are the subduction and the shallow crustal earthquakes, the results show that PGA and PSA at the YSP are more strongly affected by shallow crustal earthquakes as resulted by the Opak fault activity,
- Results from probabilistic seismic hazard analysis for the 10% PE in 50 years at YSP indicate that PSA and PSA in bed-rock upon arrival on the surface have been amplified with values close enough to the site coefficients F_a and F_v as presented in the Indonesian Seismic Code,
- In general, the distribution patterns of PGA and PSA maps for 2/3 of 2% PE in YSP are congruent, but its intensity and distribution area are higher/wider as compared to the PGA and PSA maps in the 10% PE analysis in 50 years,
- The maximum PGA and PSA values of 2/3 of 2% PE in general are greater in the range of 20 - 33% than the maximum PGA and PSA results from the analysis of 10% PE for 50 years, even though further deep investigation need to be carried out.

REFERENCES

[1] F Mulargia, P.B. Stark, R.J. Geller, Why is the Probabilistic Seismic Hazard Analysis (PSHA) still used ?, Journal of Physics of the Earth and Planetary Interiors, Vol.264, pp.63-75, (2017)

[2] L. Makrup, H.M Sodik, S.Winarno, B. Suryo, B. Sunardi, Soil Surface Hazard Map for Yogyakarta, Indonesia, Based on Probabilistic Seismic Hazard Analysis, Codes and Global V_{S30}, International Journal of Civil Engineering and Technology (IJCIET), Vol. 9, Issue 6, pp.637-648, (2018).

[3] C.J Spencer, R.A Harris, J.R Major , Provenace of Permian-Triassic Gondwana Sequence units accreted to the banda Arc in the Timor Region: Constrains from zircon U-Pb and Hf isotops, Gondwana Research 38, pp. 28-36, (2016)

[4] T.O Simanjuntak, A.J Barber, Contrasting tectonic style in the Neogene orogenic belts of Indonesia, Pennsylvania State University, (2016)

[5] R D Bertero, V V Bertero, *Performance Based Seismic Engineering: Development and Application of a Comprehensive Conceptual Approach to Design of Building*, Chapter 8 of Earthquake Engineering from Engineering Seismology to Performance Based Engineering, CRC Press, (2004)

[6] S. Pramumijoyo, M. Thant, and H. Kawase, "Seismic Hazard Mapping for Yogyakarta Dipression Area, Indonesia," 2008, pp. 54–65.

[7] M.Irsyam, S Widyantoro, D.H.Natawijaya, I.Meilano, A.Rudyanto, S.Hidayati, W.Triyoso, N.R Hanifa, D.Djarwadi, L.Faisal, Sunarjito, Peta Sumber dan Bahaya Gempa Indonesia 2017, Pusat Studi Gempa Nasional Pusat Litbang Perimahan dan Pemukiman, 376p, (2017)

[8] B Sunardi, Percepatan Tanah sintetis kota Yogyakarta berdasarkan Deagregasi Bahaya Gempa, Jounal Lingkungan dan Bencana Geologi, Vol.6, No.2, pp.211-218, (2016). (in Bahasa)

[9] T.F. Fathani, W.Wilopo, ,Seismic Microzonation studies Considering Local Site Effects for Yogyakarta City, Indonesia, International Journal of GEOMATE, Vol.12, Issue 32, pp.152-160, (2017)

[10] Badan Standardisasi Nasional, "Tata Cara Perencanaan Ketahanan Gempa Untuk Struktur Bangunan Gedung dan Non Gedung," *Sni 17262012*, p. 149, 2012.

[11] Z. L. Kyaw, S. Pramumijoyo, S. Husein, T. F. Fathani, J. Kiyono, and R. R. Putra, "Estimation of Subsurface Soil Layers using H / V Spectrum of Densely Measured Microtremor Observations (Case Study : Yogyakarta City , Central Java- Indonesia)," *Int. J. Sustain. Futur. Hum. Secur.*, vol. 2, no. 1, pp. 13–20, 2014.

[12] D. W. Nurwihastuti, J. Sartohadi, D. Mardiatno, U. Nehren, and Restu, "Understanding of Earthquake Damage Pattern through Geomorphological Approach: A Case Study of 2006 Earthquake in Bantul, Yogyakarta, Indonesia," *World J. Eng. Technol.*, vol. 2, no. 3, pp. 61–70, 2014.

[13] Daryono, "Indeks kerentanan seismik berdasarkan mikrotremor pada setiap satuan bentuk lahan di zona Graben Bantul, Daerah Istimewa Yogyakarta," Gadjah Mada University, 2011 (in Bahasa).

[14] F. Press, R. Siever , Earth, WH Freeman and Company, San Francisco, (1978)

[15] A.Kijko, Introduction to Probabilistic Seismic Hazard Analysis, Natural Hazard Centre, University of Pretoria, South Africa, 26p, (2011).

[16] J.W.Baker, Introduction to Probabilistic Seismic Hazard Analysis (PSHA), Stanford University, Version 1.3, 72p, (2008)

[17] N. Nguyen, J.Griffin, A.Cipta, P.R.Cummins, Indonesia's Historical earthquakes, Modelled Example for Improving the National Hazard Map, Geoscience Australia, 79 p., (2015)

[18] F. Febriani, Subsurface structure of the Cimandiri Fault Zone, West Java, Indonesia, PhD Thesis, Graduate School of Science, Chiba University, 163 p, (2014)

[19] B.M. Hutapea, I.Mangape, Analisis Hazard Gempa dan Usulan Ground Motion Batuan Dasar untuk Kota Jakarta, Jurnal Teknik Sipil, Institut Teknologi Bandung, Vol.16, No.3, 121-132, (2009), (in Bahasa)

[20] W.Partono, M. Irsyam, S.P.R Wardani, Development of site class and site coefficient maps of Semarang, Indonesia, using field shear wave velocity data, MATEC Web Conference, 101, 01010, (2017)

[21] H. Z. Abidin, H. Andreas, T. Kato, T. Ito, I. Meilano, F. Kimata, D.H. Natawidjaja, H. Harjono, Crustal Deformation Studies at Java, Journal of Earthquake and Tsunami, Vol.3, No.2, pp.77-88, (2009).

[22] A.Saputra, C. Gomez, I.Delikostidis, P.Z. Reza, D.S. Hatmoko, J.Sartohadi, M.A. Setiawan, Determining earthquake susceptable area southeast of Yogyakarta, Indonesia-Outcrop analysis from structure from mition (SfM) and geographic information system, Geoscience, 8, 132, doi:10.3390/geosciences8040132

[23] T. R. Walter, L.Wang,, B.G. Luchr, J. Wessermann, Y.Bechr, S.Parolai, A. Anggraini, E.Gunter, M.Sobiesiak, H.Grosser, H.U.Wetzel, C.Melkereit, P.J.K.S. Brotopuspito, P. Haryadi, J.Zschau , "The 26 May 2006 magnitude 6.4 Yogyakarta earthquake south of Mt. Merapi volcano: Did lahar deposits amplify ground shaking and thus lead to the disaster?," *Geochemistry, Geophys. Geosystems*, vol. 9, no. 5, p. n/a-n/a, May 2008.

[24] B. Sunardi, Peta deagregasi hazrd gempa Wilayah Jawa dan rekomendasi ground motion di empat kota, Master Thesis, Department of Civil Engineering, Islamic University of Indonesia, Yogyakarta, 239p, (2013) (in Bahasa)

[25] S. Akkar, M. A. Sandıkkaya, and J. J. Bommer, "Empirical ground-motion models for point- and extended-source crustal earthquake scenarios in Europe and the Middle East," *Bull. Earthq. Eng.*, vol. 12, no. 1, pp. 359–387, 2014.

[26] F. Cotton, F. Scherbaum, J. J. Bommer, and H. Bungum, "Criteria for selecting and adjusting ground-motion models for specific target regions: Application to central Europe and rock sites," *J. Seismol.*, vol. 10, no. 2, pp. 137–156, 2006.

[27] J. Douglas, E. Faccioli, F. Cotton, and C. Cauzzi, "Selection of ground-motion prediction equations for GEM1," *Earthquake*, no. September, pp. 1–3, 2009.

[28] J. J. Bommer, J. Douglas, F. Scherbaum, F. Cotton, H. Bungum, and D. Fah, "On the Selection of Ground-Motion Prediction Equations for Seismic Hazard Analysis," *Seismol. Res. Lett.*, vol. 81, no. 5, pp. 783–793, Sep. 2010.

[29] J. P. Stewart *et al.*, "Selection of ground motion prediction equations for the global earthquake model," *Earthq. Spectra*, vol. 31, no. 1, pp. 19–45, 2015.

[30] W. Pawirodikromo, The Estimated PGA map of Mw6.4 Yogyakarta, Indonesia Earthquake Constructed from the Modified Mercalli Intensity Imm, Bulletin of the New Zealand Society of Earthquake Enfineering (BNZSEE), Vol.52, Issue 2, pp.94-104, (2018).

[31] J. J. Bommer and F. Scherbaum, "Capturing and limiting ground motion uncertainty in seismic hazard assessment," *Dir. strong motion Instrum.*, vol. 58, pp. 25–40, 2005.

[32] G. M. Atkinson, “An empirical perspective on uncertainty in earthquake ground motion prediction,” *Can. J. Civ. Eng.*, vol. 38, no. 9, pp. 1002–1015, 2011.

[33] F. Strasser, J. Bommer, and N. Abrahamson, “Estimating Ground-Motion Variability: Issues, Insights & Challenges,” *14 th World Conf. Earthq. Eng.*, 2008.

[34] R. Foulser-Piggott, “Quantifying the epistemic uncertainty in ground motion models and prediction,” *Soil Dyn. Earthq. Eng.*, vol. 65, pp. 256–268, 2014.

[35] V. Sokolov, F. Wenzel, W. Y. Jean, and K. L. Wen, “Uncertainty and spatial correlation of earthquake ground motion in Taiwan,” *Terr. Atmos. Ocean. Sci.*, vol. 21, no. 6, pp. 905–921, 2010.

[36] E Delavaud, F Cotton, C. Beauval, S.Akkar, F.Scherbaum, L.Danciou, Construction of a ground motion logic tree for PSHA in Europe within the SHARE project, The 15th WCEE, Lisboa, (2012)

[37] Delavaud, E., Cotton, F., Akkar, S., Scherbaum, F., Danciu, L., Beauval, C., Drouet, S., Douglas, J., Basili, R., Sandikkaya, M. A., Segou, M., Faccioli, E., Theodoulidis, N. (2012): Toward a ground-motion logic tree for probabilistic seismic hazard assessment in Europe. - *Journal of Seismology*, *16*, 3, pp. 451—473.

[38] P. Bazzurro, A. Cornell, Ground Motion Amplification in Non-linear Soil Site with Uncertain Properties, Bulletin of the Seismological Society of America, Vol.94, No.6, pp.2090-2109, (2004).

[39] W. I. Cameroon, R.A. Green, Soil Non-linearity versus Frequency Effects, International Workshop on the Uncertainties in Non-linear Soil Properties and their Impact on Modeling Dynamic Response, pp.1-7, (2004).